Development, Growth & Differentiation
The Japanese Society of Developmental Biologists

Develop. Growth Differ. (2013) **55**, 237–246 doi: 10.1111/dgd.12023

Original Article

Identification and characterization of *Pl*Alix, the Alix homologue from the Mediterranean sea urchin *Paracentrotus lividus*

Daniele P. Romancino,[1†] Letizia Anello,[1†] Giovanni Morici,[2] Alessandra d'Azzo,[3] Antonella Bongiovanni[1*†] and Maria Di Bernardo[1†]

[1]*Institute of Biomedicine and Molecular Immunology (IBIM), National Research Council (CNR), via Ugo La Malfa, 153-90100, Palermo, Italy;* [2]*Dipartimento di Scienze e Tecnologie Molecolari e Biomolecolari (STEMBIO), Università di Palermo, Viale delle Scienze, ed., 16-90128, Palermo, Italy; and* [3]*Department of Genetics, St. Jude Children's Research Hospital, 262 Danny Thomas Place, Memphis, TN, 38105, USA*

The sea urchin provides a relatively simple and tractable system for analyzing the early stages of embryo development. Here, we use the sea urchin species, *Paracentrotus lividus*, to investigate the role of Alix in key stages of embryogenesis, namely the egg fertilization and the first cleavage division. Alix is a multifunctional protein involved in different cellular processes including endocytic membrane trafficking, filamentous (F)-actin remodeling, and cytokinesis. Alix homologues have been identified in different metazoans; in these organisms, Alix is involved in oogenesis and in determination/differentiation events during embryo development. Herein, we describe the identification of the sea urchin homologue of Alix, *Pl*Alix. The deduced amino acid sequence shows that Alix is highly conserved in sea urchins. Accordingly, we detect the *Pl*Alix protein cross-reacting with monoclonal Alix antibodies in extracts from *P. lividus*, at different developmental stages. Focusing on the role of *Pl*Alix during early embryogenesis we found that *Pl*Alix is a maternal protein that is expressed at increasingly higher levels from fertilization to the 2-cell stage embryo. In sea urchin eggs, *Pl*Alix localizes throughout the cytoplasm with a punctuated pattern and, soon after fertilization, accumulates in larger puncta in the cytosol, and in microvilli-like protrusions. Together our data show that *Pl*Alix is structurally conserved from sea urchin to mammals and may open new lines of inquiry into the role of Alix during the early stages of embryo development.

Key words: 2-cell stage embryo, Alix/AIP1, F-actin, sea urchin embryo.

Introduction

Cytoskeletal rearrangements, modulation of receptor-mediated cell signaling, and apoptosis are fundamental cellular processes involved in the early stages of animal development. In mammals Alix/AIP1 (ALG-2 interacting protein x/1) has been implicated in these diverse cellular events during cellular differentiation (Odorizzi 2006; Bongiovanni *et al.* 2012); however, until now the function/s of Alix during embryo development has not been elucidated. Alix is an evolutionarily conserved protein that derives its name from one of its interacting partners, the Apoptosis-Linked Gene-2 (ALG-2), a Ca^{++}-binding protein involved in apoptosis (Missotten *et al.* 1999; Vito *et al.* 1999). The multitasking properties of Alix rely on its tripartite protein structure that allows its interaction with a multitude of partners. This domain organization is well conserved among Alix homologues and includes the N-terminal Bro1 domain, a proline-rich C-terminal region (PRR), and a central sequence containing two coiled-coil motif (V-domain) (Fisher *et al.* 2007; Pires *et al.* 2009). By interacting with the Endosomal Sorting Complexes Required for Transport (ESCRT) I and III at the Bro1 and PRR domains, respectively, Alix synergistically coordinates the endocytosis and recycling of membrane receptors, viral budding, and cytokinesis (Katoh *et al.* 2003, 2004; Martin-Serrano *et al.* 2003; Strack *et al.* 2003; Schmidt *et al.* 2004; McCullough *et al.*

*Author to whom all correspondence should be addressed.
Email: bongiovanni@ibim.cnr.it
†All authors contributed to the acquisition, analysis and interpretation of the data.
Received 30 July 2012; revised 11 October 2012; accepted 31 October 2012.

2008). Relevant to the current study are the findings that Alix also participates in cytoskeleton remodeling by binding with F-actin at the Bro1 and PRR domains and other components of the cytoskeleton at the N-terminal half of its V-domain (Cabezas *et al.* 2005; Pan *et al.* 2006).

An Alix related protein, named ALX-1, has been detected in *Caenorhabditis elegans* and participates in the internalization and degradation of the receptor LIN-12 during patterning of the vulvar precursor cells (VPCs) (Shaye & Greenwald 2005). Similarly to its mammalian counterpart, ALX-1 is also associated with receptor recycling and the biogenesis of the multivesicular endosomes (MVEs) in the intestine (Shi *et al.* 2007). In *Drosophila melanogaster*, the Alix homologue forms a complex with the E3 ubiquitin ligase Plenty of SH3s (POSH) and ALG-2, and regulates the Jun N-terminal kinase (JNK) signal transduction pathway during the development of the imaginal eye discs (Tsuda *et al.* 2006).

Here, we explore the role of Alix in early embryogenesis, particularly at the developmental stages immediately following fertilization. We used the Mediterranean sea urchin *P. lividus* to show that Alix is conserved during evolution and that the sea urchin Alix homologue, *Pl*Alix, is expressed in unfertilized eggs and throughout early embryonic development. Furthermore, we show that the localization of *Pl*Alix changes dramatically after fertilization, becoming concentrated in specific regions. These findings suggest that *Pl*Alix may function during early developmental events, a role that the protein may also exert in mammals.

Materials and methods

Identification of Pl*Alix*

A *P. lividus* cDNA clone showing similarity to HuAlix was identified in a blast search of the *Paracentrotus lividus* expressed sequence tag (EST) database. The corresponding clone was picked up and sequenced. The sequence data have been submitted to the European Molecular Biology Laboratory (EMBL) database under accession number HE646599.

Sequence analysis, homology modeling, and phylogenetic tree construction

Amino acid sequences were aligned by the CLUSTALW program (http://www.ebi.ac.uk/Tools/msa/clustalw2). Comparative protein structure model for the *Pl*Alix sequence was generated using the MODELLER-9v4 software, based on the crystallographic structure of HuAlix Bro1 and V domains (PDB code 2OEV).

Phylogenetic trees were inferred by the neighbor-joining (NJ) method, using MEGA5 (Tamura *et al.* 2011). Reliability of branching patterns in the NJ tree were assessed by 1000 bootstrap resamplings of the alignment data (Nei & Kumar 2000). Phylogenetic tree was constructed using the sequences of Alix/Pcdc6IP homologues identified by BLASTP homology search. Analysis was conducted with proteins of 10 different *taxa*.

Egg and embryo culture

*Paracentrotous lividus s*ea urchins were collected along the north-western coast of Sicily. Gametes were harvested and eggs fertilized and cultured as previously described (Giudice 1973). Eggs used in immunostaining experiments were fertilized in the presence of 2 mmol/L PABA (para-aminobenzoic acid) to remove fertilization membrane. Total and post-nuclear proteins from eggs or embryos were extracted as previously described (Bongiovanni *et al.* 2012).

Immunoprecipitation and western blotting

60′ postfertilization embryos were lysed at 4°C for 30 min, using Hypotonic Buffer: 10 mmol/L Tris–HCl, pH 7.8, 1 mmol/L $CaCl_2$, 5 mmol/L KCl, protease inhibitor cocktail (Complete, EDTA-free; Roche), Phosphatase Inhibitor Cocktail 1 and 2 (Sigma-Aldrich). Embryos were then disrupted by Dounce homogenization (40 strokes), and cellular debris and nuclei were removed by 10 min centrifugation at 800 *g*. MG132 (5 μmol/L final concentration), N-Ethylmalemide (10 mmol/L final concentration), and 2 mmol/L CaCl2 (final concentrations) were added to 1.5 mg of post-nuclear proteins from embryos in a final volume of 1 mL. Lysates were pre-cleared by 1 h incubation at room temperature with 25 μL of protein A/G Plus agarose beads (Santa Cruz Biotechnology) and then spun at 1000 *g*. 1.5 μg of anti-Alix (clone 3A9; Santa Cruz Biotechnology) or anti-Alix (clone 1A12; Santa Cruz Biotechnology) were added to the supernatant and incubated over night at 4°C, a sample without any antibody was used as negative control. To immunoprecipitate Alix, protein A/G Plus agarose beads were added and incubated at room temperature for 2 h (Santa Cruz Biotechnology). The beads were washed five times with Hypotonic Buffer supplemented with 0.1% NP-40, and the bound proteins detached. Immunoprecipitated proteins and total protein extracts were loaded onto sodium dodecyl sulfate (SDS)polyacrylamide gel and subjected to electrophoresis at

20 mA constant current, for 1 h. Proteins were wet-transferred at 90 mA overnight onto polyvinylidene difluoride membranes (PVDF, Hybond-P; GE Healthcare). Immunoblotting was performed as described (Bongiovanni *et al.* 2012) using a purified mouse anti-AIP1/Alix (BD Biosciences), produced against mouse Alix (immunogen: aa. 375–580) diluted 1:250, or rabbit anti-polyUbiquitin (THERMO Scientific), diluted 1:250. Quantification of bands was carried out, below saturation levels, using Quantity One software (Bio-Rad, Hercules, CA, USA).

Quantitative PCR

Total RNA was isolated from unfertilized *P. lividus* eggs (UE) and embryos at different stages of development (5′, 30′, 60′, 120′ postfertilization) using TRI Reagent (Ambion), according to the manufacturer's instructions.

First strand cDNAs were retro-transcribed with SuperScript III Reverse Transcriptase (Invitrogen) using 2.5 μg of RNA. Quantitative real-time polymerase chain reaction (qPCR) was carried out on the cDNA equivalent of 8 embryos (25 ng), using Power SYBR Green Master Mix (Applied Biosystems). *Pl*Alix primers were used to obtain a 110 bp length amplicon:

AL1500for 5′ TACCAGACCATTCTCAACAAT 3′

AL1610rev 5′ TGCTATTTCCGCTTCGCTTTT 3′.

Mitochondrial cytochrome oxidase gene primers were used to obtain a 91 bp length amplicon as an endogenous reference to normalize data (Cavalieri *et al.* 2011):

Cyt-ox For2 5′ TTGGGGTTAATCTAACATTCTTC 3′:

Cyt-ox Rev2 5′ AGGGTATAGGCATCTGGATAG 3′.

qPCR experiments were carried out in triplicate using 75 nmol/L primers and a StepOnePlus Real-Time PCR System (Applied Biosystems); data were analyzed using the Applied Biosystems StepOnePlus. Real-Time PCR Software v2.1 was used in the comparative C_t method ($\Delta\Delta C_t$). The PCR cycle conditions were: initial denaturation at 95°C for 10 min, 40 cycles of 95°C for 15 s and 60°C for 1 min, and a final melting curve step.

Whole-mount immunofluorescence

Eggs and embryos were fixed in 4% paraformaldehyde in PBS (phosphate-buffered saline), washed three times in PBS, and blocked in 5% goat serum in PBS. Samples were incubated overnight a 4°C with anti-Alix (clone 3A9; Santa Cruz) diluted 1:20, or rabbit polyclonal anti-Alix (Bongiovanni *et al.* 2012) diluted 1:20 in blocking solution, washed in goat serum/PBS and incubated with Alexa Fluor 488 anti-mouse IgG (Invitrogen) or Alexa Fluor 594 anti-rabbit IgG (Invitrogen). F-actin was detected after permeabilization using 10 mmol/L fluorescein isothiocyanate (FITC)-phalloidin at room temperature for 60 min. Microtubules were labeled using monoclonal anti-α-tubulin (Sigma), diluted 1:25, and Alexa Fluor 488 anti-mouse IgG (Invitrogen) as secondary antibodies. After washing in goat serum/PBS and PBS, samples were mounted with VECTASHIELD mounting medium (Vector LAB). Specimens were examined by FluoView FV1000 confocal microscope (Olympus).

Results

*Identification, bioinformatic, and phylogenetic analyses of Pl*Alix

To identify the *P. lividus* Alix homologue, we used the human Alix (HuAlix) sequence to screen a *P. lividus* EST database containing partial sequences of a cDNA collection from unfertilized eggs and embryos (Marine Genomics Europe, NoE, project funded by European commission, FP6). The sequencing and analysis of an isolated, full length cDNA clone, from unfertilized egg cDNA library, showed that the predictive *Pl*Alix protein consists of 896 amino acid residues, with a calculated molecular weight of 98.42 kDa that is very close to HuAlix (868 aa. residues and a calculated molecular weight of 96.02 kDa). The putative *Pl*Alix has 85.5% identity compared with the predicted Alix protein of the sea urchin species, *Strongylocentrotus purpuratus*, and 45.1% identity and 63.3% similarity to its human counterpart. The multialignment of Alix homologous proteins from several *taxa* is reported in supplementary Figure S1.

To analyze the structure-function of *Pl*Alix, we generated a comparative protein structure model of *Pl*Alix based on the crystallographic structure of HuAlix Bro1 and V domains (PDB ID: 2OEV) (Fisher *et al.* 2007), using the MODELLER-9v4 software (Eswar *et al.* 2007). As in mammalian Alix proteins, the tripartite domain organization also occurs in *Pl*Alix: N-terminal Bro1 domain, central coiled-coil V domain, and C-terminal Proline Rich Domain (PRD). The elements of the sea urchin and human Alix secondary structure (beta sheets and alpha helices) have been preserved, with lesser differences in the central V domain (Fig. 1A). The two hydrophobic regions (Patch 1 and Patch 2) on the Bro1 surface (Kim *et al.* 2005; Fisher *et al.* 2007) are also conserved in the Bro1 domain of *Pl*Alix (Fig. 1A). Specifically, the docking site for the ESCRT-III component CHMP4 (charged multivesicular body protein 4) is well conserved in Patch 1, as well as the interaction domain for the SH2 of Src, within the Patch 2 around the Tyr321 (Fig. 1A). We also noted the

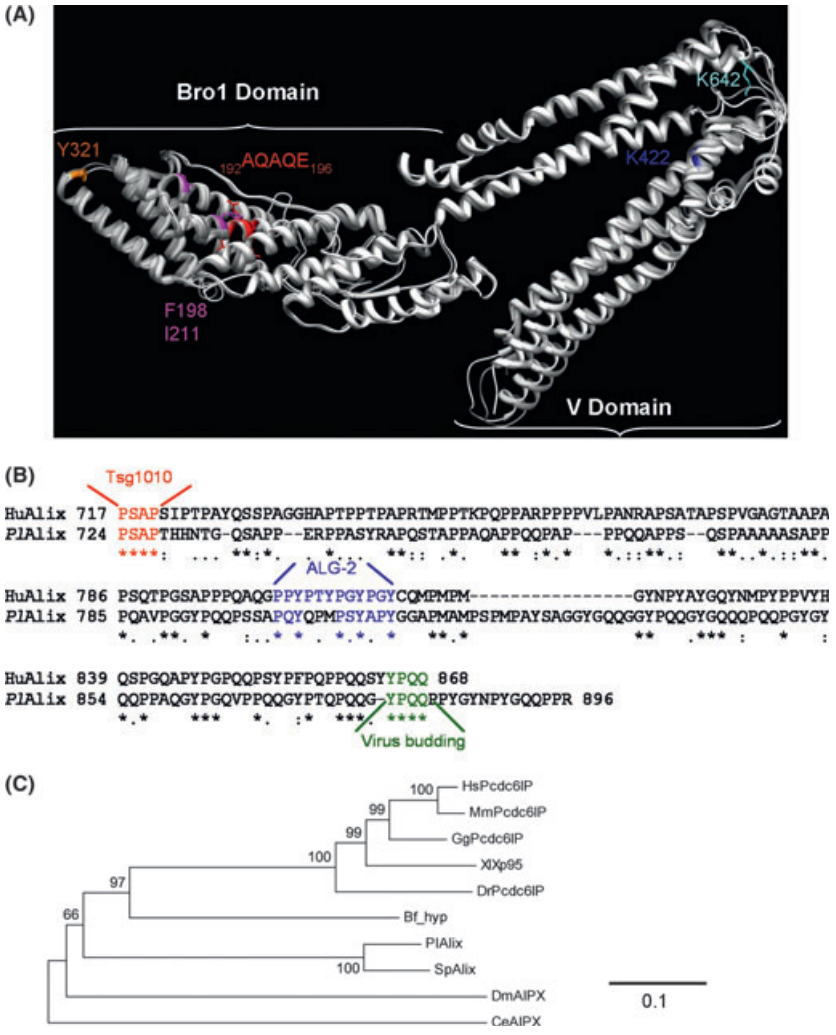

Fig. 1. Bioinformatic and phylogenetic analyses of *Pl*Alix (A) Homology model of *Pl*Alix Bro1 and V domains. Superimposition of the crystal structure of HuAlix Bro1 and V domains (PDB identity code 2OEV, gray cartoon) and the model of the *Pl*Alix domains (white cartoon) predicted by MODELLER program. Color scheme of the residues preserved between the human and *Paracentrotus lividus* Alix sequences are indicated, and numbered for the *Pl*Alix sequence. In Bro1 domain: residues involved in CHMP4 interaction (magenta); the domain-binding sites for Kinase A (red) and Src SH2 (orange). The conserved two hydrophobic regions, within the Bro1 domain, are around the docking sites for CHMP4 (Patch 1) and for Src (Patch 2). In V domain: K642 (cyan), within the hinge region, and K422 (blue). The molecular graphic image was produced using the UCSF Chimera program (http://www.cgl.ucsf.edu/chimera). (B) Sequence comparison of the human and *P. lividus* Alix proline rich domain (PRD) domains. Matching HuAlix/*Pl*Alix residues essential to promote interaction with the ESCRT-I subunit TSG101 (red), ALG-2 (blue), and virus budding (green), are indicated. (C) Phylogenetic tree of Alix. Neighbor-joining tree made with the alignment of Alix Bro1-V domain from the following selected taxa: *Chordata*, *Homo sapiens* (Hs: NP_037506.2), *Mus musculus* (Mm: AAH26823.1), *Gallus gallus* (Gg:NP_001026164.1), *Xenopus laevis* (Xl: NP_001081870.1), *Danio rerio* (Dr: NP_998525.2); *Cephalochordata*, *Branchiostoma floridae* (Bf: XP_002609564.1); *Echinodermata*, *Paracentrotus lividus* (Pl: HE 646599) and *Strongylocentrotus purpuratus* (Sp: XP_001204017.1); *Arthropoda*, *Drosophila melanogaster* (Dm: NP_651582.1); and *Nematoda*, *Caenorhabditis elegans* (Ce: NP_001022713.1). Numbers at the nodes indicate distances between groups of sequences as determined by bootstrap analysis (1000 bootstrap replicates).

presence of a conserved motif considered a putative Kinase A phosphorylation site (Mattei *et al.* 2005) and of a conserved region within the "hinge region" of the *Pl*Alix V domain (Pires *et al.* 2009). Within the PRD domain (Fig. 1B), the amino acid residues that are known to be important for interactions with the ESCRT-I protein TSG101 (tumor susceptibility gene 101 protein), ALG-2 and the two retroviral Gag proteins (P6 and P9) (Odorizzi 2006), are also well conserved between HuAlix and *Pl*Alix.

Phylogenetic analysis was performed using Alix homologues from different species. Alix homologues

were identified by BLASTP search and downloaded from the GenBank database. Amino acid sequences were aligned by the CLUSTALW program and complete alignments are shown in Figure S1. Due to the low degree of conservation, the phylogenetic tree was reconstructed excluding the highly variable C-terminal PRD domain. Analysis was first conducted either with the Bro1 or the central V domain (data not shown), and ultimately with the whole region containing both domains (Fig. 1C). The topology of the tree and the high bootstrap values confirm that Alix from *Echinodermata* and *Chordata* share a common ancestor and that *D. melanogaster* and *C. elegans* Alix diverged earlier. Moreover, if compared with the *Protostomes* Alix, sea urchins Alix is closer to *Chordates* both in terms of topology and evolutionary distance expressed as the number of amino acid differences per site.

Identification and temporal expression of Pl*Alix in* P. lividus *embryos*

To identify the *Pl*Alix protein, western blots were performed using protein extracts from fertilized eggs and from mouse C2C12 muscle cells, used as positive control (Bongiovanni *et al.* 2012); denatured proteins were immunoblotted using a commercially available mouse monoclonal anti-Alix antibody (BD Biosciences). As shown in Figure 2A, a band of the expected molecular weight (about 100 kDa) comigrates with the mouse Alix protein present in C2C12 protein extract. To confirm the identity of *Pl*Alix, native proteins from post-nuclear *P. lividus* fertilized eggs were immunoprecipitated using two additional anti-Alix monoclonal antibodies, in the presence of the proteasome inhibitor, MG132, and the de-ubiquitinating enzyme inhibitor, N-Ethylmalemide. Immunoblotting of these immunoprecipitated proteins confirmed the presence of a band corresponding to the *Pl*Alix antigen in the *P. lividus* protein extracts (Fig. 2B). Immunoprecipitation of *Pl*Alix was more efficiently driven by monoclonal antibody clone 3A9 than 1A12, which were both conformation-sensitive monoclonal antibodies raised against the full length HuAlix (Pan *et al.* 2006, 2008). This difference in efficiency may depend on the differential affinity of the two antibodies to the native *Pl*Alix. Other bands at higher molecular weights were also immunoprecipitated with the two anti-Alix antibodies and, in line with the preservation of at least one putative ubiquitination site in *Pl*Alix; they probably are ubiquitinated forms of Alix (see asterisks in Fig. 2B). This assumption is corroborated by the detection of bands with the same molecular weight using an anti-polyubiquitin antibody in immunoblots of the anti-Alix immunoprecipitates (Fig. 2B, right panel). In addition, the relative ratios of *Pl*Alix versus ubq-*Pl*Alix forms differ significantly between 1A12- and 3A9-pulled-down samples; this difference can reflect the exposure of specific epitopes in ubiquitinated forms of *Pl*Alix. It is worth noting that bands of similar size, positive for polyUbiquitin, were also detected in anti-Alix immunoprecipitates of C2C12 protein extracts, and that Alix undergoes efficient ubiquitination by three different ubiquitin ligases, including Ozz-E3 (Bongiovanni *et al.* 2012).

To analyze the expression pattern of *Pl*Alix during the early stages of development, equal amounts of protein extract from unfertilized eggs and embryos at different times following fertilization (1, 5, 15, 30, 60 and 120 min) were immunoblotted using monoclonal anti-Alix; immuno-positive Alix bands were quantified and normalized against the Ponceau S loading control. As shown in a representative gel and in the quantitative analysis of *Pl*Alix bands (Fig. 2C, D), a significant increase of *Pl*Alix protein was observed from unfertilized eggs until 60–120 min after fertilization, indicating a regulated expression during these early stages of development. In these experiments, *Pl*Alix bands are associated with lower molecular mass bands that may be cleavage products of *Pl*Alix (Fig. 2C, gray arrowhead), in line with what has been reported for HuAlix (Pan *et al.* 2008). Furthermore, immunoblots of protein extract from embryos at later developmental stages (128-cell, blastula, and gastrula stage embryos) showed that *Pl*Alix is present and its level remains unaltered during these later stages (Fig. 2E). To see if *Pl*Alix expression was similarly regulated at the transcriptional level, we analyzed the relative abundance of the *Pl*Alix transcript in unfertilized eggs (UE) and embryos up to 120′. Total RNA from each stage was retro-transcribed and used in qPCR for *Pl*Alix transcripts, normalized with cytochrome oxidase (Cavalieri *et al.* 2011). Our results show that, in contrast to protein expression, *Pl*Alix mRNA level decreased to <20% in 5′ post-fertilization embryos compared to the unfertilized eggs, and remained at low levels in all the examined developmental stages (Fig. 2F).

Subcellular localization of Pl*Alix during* P. lividus *development, from zygote to 2-cell stage embryo*

To examine the subcellular distribution of *Pl*Alix in the *P. lividus* embryo, we performed whole-mount immunofluorescence labeling of eggs and early embryos soon after fertilization (15 and 60 min). Unfertilized eggs displayed a punctuated staining of *Pl*Alix throughout the cytosol (Fig. 3A, E). In early embryos *Pl*Alix accumulated throughout the cytosol and localized in enlarged puncta near the nuclei, along the spindle microtubules (Fig. 3B, C, K, L, and M). Thus,

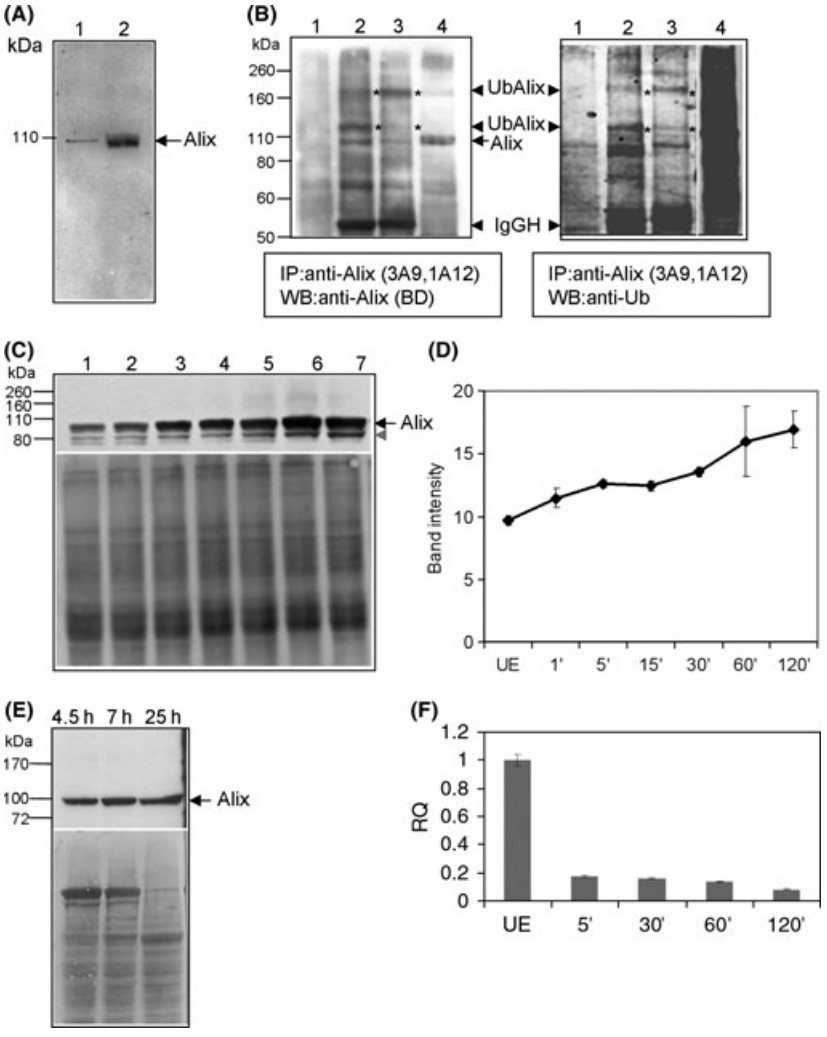

Fig. 2. Characterization and expression of *Pl*Alix (A) Immunoblot assay of denatured total proteins extracted from mouse C2C12 muscle cells (7 μg, lane 1) and fertilized eggs (60 μg, lane 2), using a monoclonal anti-Alix antibody. (B) Anti-Alix or anti-Ubiquitin immunoblot assay of post-nuclear proteins from fertilized eggs immunoprecipitated using anti-Alix clone 3A9 (lane 2) and 1A12 (lane 3), in the presence of MG132 and N-Ethylmalemide. Immunoprecipitation negative control (without antibodies) was loaded in lane 1, and post-nuclear proteins from fertilized eggs were loaded in lane 4 (20 μg). (C) Immunoblot assay of proteins from: unfertilized eggs (lane 1), embryos 1, 5, 15, 30, 60, and 120 min after fertilization (lanes 2–7). Ponceau S stained blot is shown as loading control. Gray arrowhead indicates putative cleavage products of *Pl*Alix. (D) Quantitative analysis of protein expression from unfertilized eggs to 120 min embryo stage. Quantification of bands, normalized against the corresponding Ponceau S staining, was executed using Quantity One software. Data were reported as band intensity for each sample, and were shown as means ± standard deviation of three independent experiments. (E) Immunoblot assay of proteins from embryos at 4.5 h (128 cell-stage), 7 h (blastula stage), and 25 h (gastrula stage) after fertilization. Ponceau S stained blot is shown as loading control. (F) Relative expression of *Pl*Alix mRNA at early developmental stages. cDNA from total RNA of unfertilized eggs (UE) and early stages (5′, 30′, 60′, and 120′ postfertilization) were amplified. *Pl*Alix mRNA is represented as Quantity Relative (RQ) to UE and normalized with cytochrome oxidase transcript. All error bars (SD) are derived from three experiments.

*Pl*Alix is localized in cellular structures, likely intracellular vesicles, of different sizes: the smallest are also present in unfertilized eggs, while others of larger size appear soon after fertilization and are more evident after the first division.

Close inspection of several specimens pointed out that a number of *Pl*Alix-positive structures are localized close to the cortex or extended from the membrane surface (see arrowheads in Fig. 3E–G); the number of these sub-cellular compartments increased after fertilization (Fig. 3F, G versus E panel). In order to shed light on the identity of these Alix-positive regions, we investigated on Alix localization in relation to actin-containing structures. We observed that *Pl*Alix is in close

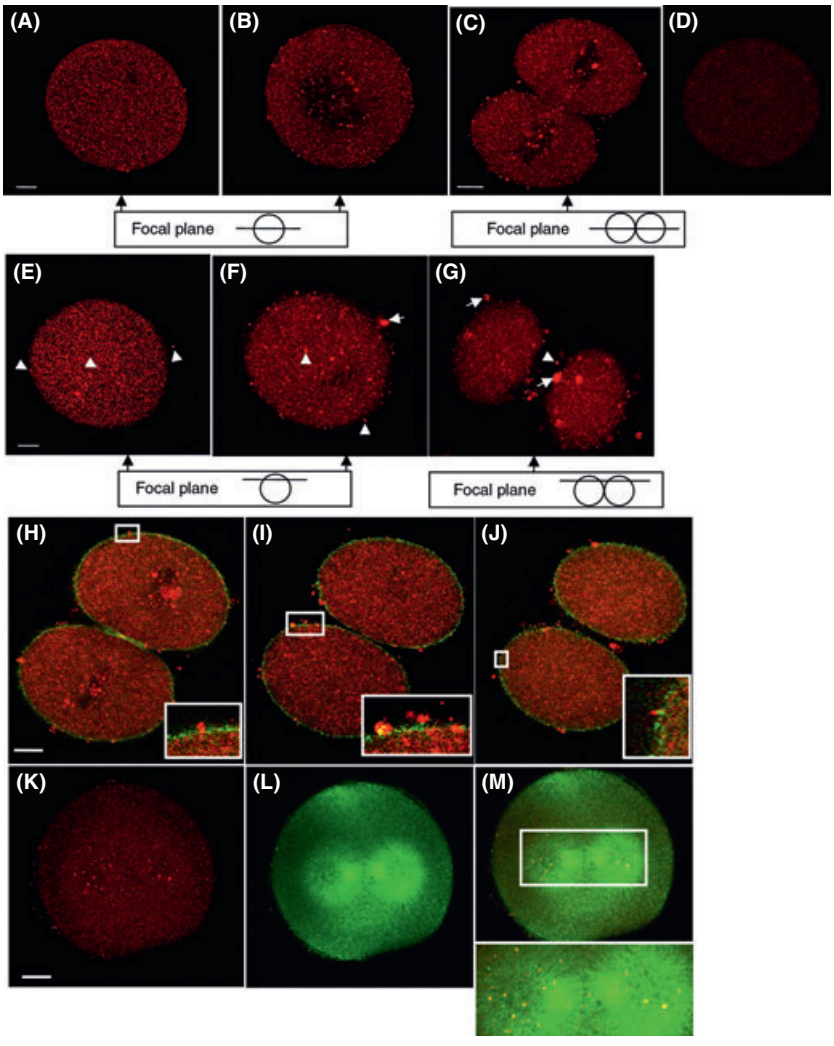

Fig. 3. Immunolocalization of *Pl*Alix protein in unfertilized eggs and 2-cell embryos. *Pl*Alix staining in unfertilized eggs (A, E), and embryos 15 (B, F) and 60 (C, G–J) min after fertilization. Images of individual sections in A–D and E–G correspond to two different meridian planes. Control of immunofluorescence with an unrelated mouse antibody is shown in D. F-actin is labeled with phalloidin- fluorescein isothiocyanate (FITC); images of individual sections and their insets at greater magnification are shown (H–J). The insets show microvilli at higher magnification, where *Pl*Alix and F-actin are juxtaposed. A single confocal section is shown, where *Pl*Alix is labeled in red, (K) and α-tubulin in green (L). Corresponding merged image (M) is shown with inset at greater magnification. The bar indicates 10 μm.

proximity with F-actin in several cellular protrusions which resemble microvilli (H–J). Furthermore, we observed that *Pl*Alix staining increased in intensity and distance from the membrane surface after fertilization and until 60 min post-fertilization.

Discussion

Cellular events such as membrane trafficking, endocytosis/exocytosis and the remodeling of actin filaments are fundamental processes during oogenesis, fertilization, and early embryogenesis. While the function of Alix has been established in all these phenomena, in differentiated mammalian cells (Odorizzi 2006; Bongiovanni *et al.* 2012), until now nothing it is known about its function/s during the early stages of embryo development. In this study, we used the Mediterranean sea urchin species, *P. lividus*, as the animal system to investigate the role of Alix in key stages of embryogenesis, namely the egg fertilization and the first cleavage division. We provide evidence for the presence of Alix in sea urchin, by comparing human Alix sequences against EST databases of the *Paracentrotus lividus* species. The sequencing and the analysis of the isolated cDNA clone confirmed this evidence. Immunoblotting, immunoprecipitation, homology modeling and phylogenetic analyses also showed that the protein *Pl*Alix is well conserved during evolution. In this context, it is worth noting that a region of similarity was indicated by the three dimensional structure of the highly hydrophobic pocket within the "hinge region" of the *Pl*Alix V-domain (Pires *et al.* 2009); this region, around Lys642 in *Pl*Alix, is well preserved. This finding suggests that *Pl*Alix might have preserved an activation/localization mechanism as the mammalian Alix. Indeed, it has been recently suggested that opening of the 'hinge region' of Alix, by posttranslational modifications and/or ligand binding, would expose different

binding sites and consequently modify the function and subcellular localization of Alix (Fisher *et al.* 2007; Zhai *et al.* 2011). In line with this concept, we have recently found that the substrate-recognition module of the Ozz-E3 ubiquitin ligase, Ozz, binds to and ubiquitinates Alix, affecting the conformation of Alix and controlling its local concentration at sites where cytoskeleton remodeling is taking place (Bongiovanni *et al.* 2012). In this regard, it is noteworthy that the preserved Lys642 of *Pl*Alix is included in the "hinge region" of the V-domain (Fig. 1A). According to the predictor of ubiquitination sites, UbPred (Radivojac *et al.* 2010), this lysine, together with six others (Lys146, Lys411, Lys422, Lys468, Lys471, Lys709), is predicted to be an ubiquitination site with more than "medium confidence". Furthermore, the finding that the putative ubiquitinated Lys642, together with Lys422 and Lys709, is well-preserved among different species makes it very attractive as a possible regulation site for the conformation and function of Alix.

Next, we examined the expression pattern of *Pl*Alix during the early stages of development. The gradual increase of the *Pl*Alix protein level immediately after fertilization and until the 2-cell stage points to a possible active role of Alix in early embryo development. In contrast, we observed a severe decrease in *Pl*Alix mRNA abundance during these early stages of development, probably as a result of the general maternal-to-zygotic transition and the loss of maternal mRNAs (Aguirre-Armenta *et al.* 2011). Taken together, these results are in agreement with the elevated efficiency of protein synthesis after fertilization (Metafora *et al.* 1971; Raff *et al.* 1981). Furthermore, protein stability could be another factor that would contribute to the overall abundance of *Pl*Alix in early developmental stages.

The immunofluorescence experiments revealed that the cytosolic staining of *Pl*Alix was noticeably remodeled if we compared eggs and early embryos; it gradually switched from diffuse and punctuated to mostly punctuated, with an increase in the number of larger spots soon after fertilization. These *Pl*Alix-positive large spots appeared 15 min after fertilization and become more evident at the first embryonic cleavage; they were distributed near the two nuclei, specifically in the central region along the spindle microtubules. This localization is in agreement with what is already known about the distribution of Alix in vesicles of endocytic trafficking in different species, from *Dictyostelium* to mammalians (Mattei *et al.* 2005; Shaye & Greenwald 2005; Montagnac *et al.* 2008). The subcellular distribution of *Pl*Alix is also compatible with the presence of a large number of small, maternally stored granules and vesicles randomly distributed in sea urchin unfertilized eggs (Ramos *et al.* 2010). Furthermore, the redistribution of cytoplasmic components upon fertilization is a common phenomenon in a variety of animal eggs and also in sea urchins, in which a whole spectrum of acidic organelles and intracellular vesicles are present (Morgan 2011). These cellular compartments are engaged in a highly organized series of vesicular transport mechanisms that are activated at different times (Matese *et al.* 1997; Conner & Wessel 1998). Among these vesicles, small endosomes are already present in the unfertilized egg, even though endocytosis is slow and possibly constitutive (Covian-Nares *et al.* 2008). Following the massive exocytosis at fertilization, the regulated compensatory endocytosis pathway takes place; it is promptly able to retrieve the excess cortical granule membranes and generate large endosomes, up to 3 μm in diameter (Whalley *et al.* 1995). Within this context, the localization of *Pl*Alix in presumptive small and large endocytic vesicles suggests that its presence is in both constitutive endosomes (small vesicles) and compensatory endosomes (large vesicles). The presence in *Pl*Alix of a well-conserved domain needed to bind with the ESCRT-III protein, CHMP4, is further evidence that Alix is likely to play an active role in endosomal functioning during development.

We and others have reported that Alix regulates the F-actin cytoskeleton and membrane dynamics during both endocytosis and the formation of cellular protrusions (Odorizzi 2006; Bongiovanni *et al.* 2012). The presence of discrete microvilli-like regions positive for *Pl*Alix in close proximity to the membrane surface or protruding from it, suggests a possible role of *Pl*Alix in the biogenesis and dynamics of egg/embryo microvilli. Microvilli are thousands of finger-like protrusions, which contain an internal ultrastructure of actin filament bundles, and cover the egg surface (Burgess & Schroeder 1977; Schroeder 1978). We observed that *Pl*Alix staining increased in intensity and distance from the membrane surface after fertilization and until 60 min postfertilization. This is in accordance to what was previously reported, that microvilli covering the surface of unfertilized eggs increase in extent and diameter between 30 and 90 min after fertilization (Schroeder 1978). A further insight about the identity of the *Pl*Alix-positive protrusions is the finding that *Pl*Alix and F-actin staining are colocalized or juxtaposed in some regions of the plasma membrane or protruding from it in the extracellular space. This colocalization is consistent with the ability of Alix to interact with both F-actin and membrane components (e.g., endophilin) (Odorizzi 2006). However, while the function of Alix has been established in differentiated mammalian cells and it has only been inferred for very late stages of embryo development (Shaye & Greenwald 2005;

Odorizzi 2006; Tsuda *et al.* 2006), our data indicate, for the first time, a role of Alix during early embryo development, namely from fertilization to the 2-cell stage embryo. Indeed, based on our findings and on what is already known about mammalian Alix, we infer that *Pl*Alix may play a function as a regulator of early developmental events, such as the biogenesis of microvilli and the endocytic pathway, a role that the protein may also exert during mammalian early embryogenesis. Thus, we believe that this work may provide new insights into the fundamental mechanisms involved in early embryo development, in particular from fertilization to the 2-cell stage.

Acknowledgments

We thank Dr Maria Ina Arnone (SZN, Naples) for keeping the cDNA libraries and providing the *Pl*Alix containing clone. Dr Yvan Campos (St. Jude C.R.H., Memphis, USA) for helpful discussion and Dr Xiaohui Qiu (St. Jude C.R.H., Memphis, USA) for the purification of the rabbit polyclonal anti-Alix antibody. We thank Dr Richard Burket for editing the manuscript. We also thank Dr Rosalia La Tona for her contribution to the qPCR experiments. This work has been partially supported by a grant from the Italian Ministry of Economy and Finance to the CNR for the Project FaReBio di Qualità.

References

Aguirre-Armenta, B., Lopez-Godınez, J., Martınez-Cadena, G. & Garcıa-Soto, J. 2011. Rho-kinase in sea urchin eggs and embryos. *Develop. Growth Differ.* **53**, 704–714.

Bongiovanni, A., Romancino, D. P., Campos, Y., Paterniti, G., Qiu, X., Moshiach, S., Di Felice, V., Vergani, N., Ustek, D. & d'Azzo, A. 2012. Alix is a Substrate of the Ozz-E3 Ligase, and Modulates Actin Remodeling in Skeletal Muscle. *J. Biol. Chem.* **287**, 12159–12171.

Burgess, D. R. & Schroeder, T. E. 1977. Polarized bundles of actin filaments within microvilli of fertilized sea urchin eggs. *J. Cell Biol.* **74**, 1032–1037.

Cabezas, A., Bache, K. G., Brech, A. & Stenmark, H. 2005. Alix regulates cortical actin and the spatial distribution of endosomes. *J. Cell Sci.* **118**, 2625–2635.

Cavalieri, V., Guarcello, R. & Spinelli, G. 2011. Specific expression of aTRIM-containing factor in ectoderm cells affects the skeletal morphogenetic program of the sea urchin embryo. *Development* **138**, 4279–4290.

Conner, S. & Wessel, G. M. 1998. Rab3 mediates cortical granule exocytosis in the sea urchin egg. *Dev Biol.* **203**, 334–344.

Covian-Nares, J. F., Smith, R. M. & Vogel, S. S. 2008. Two independent forms of endocytosis maintain embryonic cell surface homeostasis during early development. *Dev. Biol.* **316**, 135–148.

Eswar, N., Webb, B., Marti-Renom, M. A., Madhusudhan, M. S., Eramian, D., Shen, M. Y., Pieper, U. & Sali, A. 2007. Comparative protein structure modeling using MODELLER. *Curr. Protoc. Protein Sci.* Chapter 2, Unit 2.9.

Fisher, R. D., Chung, H. Y., Zhai, Q., Robinson, H., Sundquist, W. I. & Hill, C. P. 2007. Structural and biochemical studies of ALIX/AIP1 and its role in retrovirus budding. *Cell* **128**, 841–852.

Giudice, G. 1973. *Developmental Biology of the Sea Urchin Embryo*. New York and London: Academic Press.

Katoh, K., Shibata, H., Suzuki, H., Nara, A., Ishidoh, K., Kominami, E., Yoshimori, T. & Maki, M. 2003. The ALG-2-interacting Protein Alix Associates with CHMP4b, a Human Homologue of Yeast Snf7 That Is Involved in Multivesicular Body Sorting. *J. Biol. Chem.* **278**, 39104–39113.

Katoh, K., Shibata, H., Hatta, K. & Maki, M. 2004. CHMP4b is a major binding partner of the ALG-2-interacting protein Alix among the three CHMP4 isoforms. *Arch. Biochem. Biophys.* **421**, 159–165.

Kim, J., Sitaraman, S., Hierro, A., Beach, B. M., Odorizzi, G. & Hurley, J. H. 2005. Structural basis for endosomal targeting by the Bro1 domain. *Dev. Cell* **8**, 937–947.

Martin-Serrano, J., Yarovoy, A., Perez-Caballero, D. & Bieniasz, P. D. 2003. Divergent retroviral late-budding domains recruit vacuolar protein sorting factors by using alternative adaptor proteins. *Proc. Natl Acad. Sci. USA* **100**, 12414–12419.

Matese, J. C., Black, S. & Mc Clay, D. R. 1997. Regulated Exocytosis and Sequential Construction of the Extracellular Matrix Surrounding the Sea Urchin Zygote. *Dev. Biol.* **186**, 16–26.

Mattei, S., Ryves, W. J., Blot, B., Sadoul, R., Harwood, A. J., Satre, M., Klein, G. & Aubry, L. 2005. Dd-Alix, a conserved endosome-associated protein, controls Dictyostelium development. *Dev. Biol.* **279**, 99–113.

McCullough, J., D. Fisher, R., Whitby, F. G., Sundquist, W. I. & Hill, C. P. 2008. ALIX-CHMP4 interactions in the human ESCRT pathway. *Proc. Natl Acad. Sci. USA* **105**, 7687–7691.

Metafora, S., Felicetti, L. & Gambino, R. 1971. The Mechanism of Protein Synthesis Activation After Fertilization of Sea Urchin Eggs. *Proc. Natl Acad. Sci. USA* **68**, 600–604.

Missotten, M., Nichols, A., Rieger, K. & Sadoul, R. 1999. Alix, a novel mouse protein undergoing calcium-dependent interaction with the apoptosis-linked-gene 2 (ALG-2) protein. *Cell Death Differ.* **6**, 124–129.

Montagnac, G., Echard, A. & Chavrie, P. 2008. Endocytic traffic in animal cell cytokinesis. *Curr. Opin. Cell Biol.* **20**, 454–461.

Morgan, A. J. 2011. Sea urchin eggs in the acid reign. *Cell Calcium* **50**, 147–156.

Nei, M. & Kumar, S. 2000. *Molecular Evolution and Phylogenetics*. New York: Oxford University Press.

Odorizzi, G. 2006. The multiple personalities of Alix. *J. Cell Sci.* **119**, 3025–3032.

Pan, S., Wang, R., Zhou, X., He, G., Koomen, J., Kobayashi, R., Sun, L., Corvera, J., Gallick, G. E. & Kuang, J. 2006. Involvement of the conserved adaptor protein Alix in actin cytoskeleton assembly. *J. Biol. Chem.* **281**, 34640–34650.

Pan, S., Wang, R., Zhou, X., Corvera, J., Kloc, M., Sifers, R., Gallick, G. E., Lin, S. H. & Kuang, J. 2008. Extracellular Alix regulates integrin-mediated cell adhesions and extracellular matrix assembly. *EMBO J.* **27**, 2077–2090.

Pires, R., Hartlieb, B., Signor, L., Schoehn, G., Lata, S., Roessle, M., Moriscot, C., Popov, S., Hinz, A., Jamin, M., Boyer, V., Sadoul, R., Forest, E., Svergun, D. I., Göttlinger, H. G. & Weissenhorn, W. 2009. A crescent-shaped ALIX dimer targets ESCRT-III CHMP4 filaments. *Structure* **17**, 843–856.

Radivojac, P., Vacic, V., Haynes, C., Cocklin, R. R., Mohan, A., Heyen, J. W., Goebl, M. G. & lakoucheva, L. M. 2010. Identification, analysis, and prediction of protein ubiquitination sites. *Proteins* **78**, 365–380.

Raff, R. A., Brandis, J. W., Huffman, C. J., Koch, A. L. & Leister, D. E. 1981. Protein synthesis as an early response to fertilization of the sea urchin egg: a model. *Dev. Biol.* **86**, 265–271.

Ramos, I. B., Miranda, K., Pace, D. A., Verbist, K. C., Lin, F. Y., Zhang, Y., Oldfield, E., Machado, E. A., De Souza, W. & Docampo, R. 2010. Calcium- and polyphosphate-containing acidic granules of sea urchin eggs are similar to acidocalcisomes, but are not the targets for NAADP. *Biochem. J.* **429**, 485–495.

Schmidt, M. H., Hoeller, D., Yu, J., Furnari, F. B., Cavenee, W. K., Dikic, I. & Bögler, O. 2004. Alix/AIP1 antagonizes epidermal growth factor receptor downregulation by the Cbl-SETA/CIN85 complex. *Mol. Cell Biol.* **24**, 8981–8993.

Schroeder, T. E. 1978. Microvilli on Sea Urchin Eggs: a Second Burst of Elongation. *Dev. Biol.* **64**, 342–346.

Shaye, D. D. & Greenwald, I. 2005. LIN-12/Notch trafficking and regulation of DSL ligand activity during vulval induction in *Caenorhabditis elegans*. *Development* **132**, 5081–5092.

Shi, A., Pant, S., Balklava, Z., Chen, C. C., Figueroa, V. & Grant, B. D. 2007. A novel requirement for *C. elegans* Alix/ALX-1 in RME-1 mediated membrane transport. *Curr. Biol.* **17**, 1913–1924.

Strack, B., Calistri, A., Craig, S., Popova, E. & Gottlinger, H. G. 2003. AIP1/ALIX is a binding partner for HIV-1 p6 and EIAV p9 functioning in virus budding. *Cell* **114**, 689–699.

Tamura, K., Peterson, D., Peterson, N., Stecher, G., Nei, M. & Kumar, S. 2011. MEGA5: molecular evolutionary genetics analysis using maximum likelihood, evolutionary distance, and maximum parsimony methods. *Mol. Biol. Evol.* **28**, 2731–2739.

Tsuda, M., Seongc, K. & Aigakia, T. 2006. POSH, a scaffold protein for JNK signaling, binds to ALG-2 and ALIX in Drosophila. *FEBS Lett.* **580**, 3296–3300.

Vito, P., Pellegrini, L., Guiet, C. & D'Adamio, L. 1999. Cloning of AIP1, a novel protein that associates with the apoptosis-linked gene ALG-2 in a Ca2 + -dependent reaction. *J. Biol. Chem.* **274**, 1533–1540.

Whalley, T., Terasaki, M., Cho, M. S. & Vogel, S. S. 1995. Direct Membrane Retrieval into Large Vesicles After Exocytosis in Sea Urchin Eggs. *J. Cell Biol.* **131**, 1183–1192.

Zhai, Q., Landesman, M. B., Chung, H. Y., Dierkers, A., Jeffries, C. M., Trewhella, J., Hill, C. P. & Sundquist, W. I. 2011. Activation of the retroviral budding factor ALIX. *J. Virol.* **85**, 9222–9226.

Supporting Information

Additional Supporting Information may be found in the online version of this article:

Fig. S1. Multi-alignment of the primary amino-acid sequence of Alix homologous proteins.